Classical correlation and quantum discord in critical systems

M. S. Sarandy*
Instituto de Física, Universidade Federal Fluminense, Av. Gal. Milton Tavares de Souza s/n, Gragoatá, Niterói 24210-346, RJ, Brazil
(Received 8 May 2009; published 12 August 2009)

We discuss the behavior of quantum and classical pairwise correlations in critical systems, with the quantumness of the correlations measured by the quantum discord. We analytically derive these correlations for general real density matrices displaying Z_2 symmetry. As an illustration, we analyze both the *XXZ* and the transverse field Ising models. Finite size as well as infinite chains are investigated and the quantum criticality is discussed. Moreover, we identify the spin functions that govern the correlations. As a further example, we also consider correlations in the Hartree-Fock ground state of the Lipkin-Meshkov-Glick model. It is then shown that both classical correlation and quantum discord exhibit signatures of the quantum phase transitions.

DOI: 10.1103/PhysRevA.80.022108 PACS number(s): 03.65.Ud, 03.67.Mn, 75.10.Jm

I. INTRODUCTION

The concept of correlation, i.e., information of one system about another, is a key element in many-body physics. Indeed, the properties of a many-body system are strongly affected by changes in the correlations among its constituents. These changes are responsible for the occurrence of remarkable phenomena, such as a quantum phase transition (QPT), which is a critical change in the ground state of a quantum system due to level crossings in its energy spectrum. QPTs occur at low temperatures T, where the de Broglie wavelength is greater than the correlation length of the thermal fluctuations (effectively $T=0$) [1,2]. Striking examples of QPTs include metal-insulator transitions in strongly correlated electronic materials, magnetic transitions in quantum spin-lattices, superfluid-Mott insulator transitions in atomic gases induced by a Bose-Einstein condensation, among others.

Correlations can be both from classical and quantum sources. The existence of genuinely quantum correlations can be usually inferred by the presence of entanglement among parts of a system. Indeed, entanglement displays a rather interesting behavior at QPTs [3], being able to indicate a quantum critical point (QCP) through nonanalyticities inherited from the ground-state energy [4,5]. Moreover, for one-dimensional critical systems, ground-state entanglement entropy exhibits a universal logarithmic scaling governed by the central charge of the Virasoro algebra associated with the underlying conformal field theory [6–8]. Remarkably, the logarithmic scaling is robust against disorder [9–12]. In higher dimensions, entanglement usually scales following an area law for noncritical systems (see, e.g., Ref. [13]). For critical models, violations of the area law have been found [14,15], with logarithmic-type corrections appearing. More recently, it has been observed that an area law is generally implied by a finite correlation length when measured in terms of the mutual information [16]. This remarkable behavior of entanglement at criticality is indeed a consequence of the correlation pattern exhibited by the ground state of the system.

Nevertheless, although entanglement provides a route to find out the existence of quantum correlations, it can be shown that they can appear even when entanglement is absent [17,18]. Quantum correlations, which can be measured by the *quantum discord* [17], often arise as a consequence of coherence in a quantum system, being present even for separable states. Moreover, entangled states commonly involve more than only quantum correlations, i.e., they usually carry classical correlations among their parts. In a multiparty mixed-state scenario, the possibility of nonseparable states with purely quantum correlations (with no supporting background of classical correlations) have also been investigated [19], but genuine indicators of multiparticle classical correlations are still under debate [20]. By focusing on condensed-matter systems, the aim of this work is, starting from an arbitrary Z_2-symmetric model, to investigate pairwise correlations, explicitly splitting up their classical and quantum contributions and analyzing their behavior at QPTs. As an illustration, ground states of both *XXZ* and transverse field Ising spin chains will be shown to share quantum as well as classical correlations for nearest-neighbor spin pairs, with both of them signaling the critical behavior of the system. An analysis of such correlations for the thermodynamic limit of *XXZ* and Ising chains has recently appeared in Ref. [21]. Here, we generalize this analysis by providing analytical expressions for the correlations in each model and also by discussing their finite-size behavior. As a further illustration, we describe the correlations in the Hartree-Fock (HF) ground state of many-body systems, taking the Lipkin-Meshkov-Glick (LMG) model as an example.

The paper is organized as follows. In Sec. II, we review the evaluation of correlations from the point of view of information theory, describing—in particular—the concept of quantum discord. In Sec. III, we discuss the computation of classical and quantum correlations for general models displaying Z_2 symmetry. Sections IV–VI are devoted to illustrating our results for the *XXZ* chain, the transverse field Ising chain, and the LMG model, respectively. Conclusions are then presented in Sec. VII.

II. CLASSICAL CORRELATIONS AND QUANTUM DISCORD

In classical information theory, the information obtained, on average, after knowing the value of a random variable X,

*msarandy@if.uff.br

which takes values within a set of probabilities $\{p_x\}$, can be quantified by its Shannon entropy $H(X)=-\Sigma_x p_x \log p_x$. We use the symbol log as denoting logarithm at base 2 throughout the text. By taking two such random variables X and Y, we can measure the correlation between them by their mutual information,

$$\mathcal{I}(X:Y) = H(X) + H(Y) - H(X,Y), \tag{1}$$

where $H(X,Y)=-\Sigma_{x,y} p_{xy} \log p_{xy}$ is the joint entropy for X and Y. By introducing the conditional entropy,

$$H(X|Y) = H(X,Y) - H(Y), \tag{2}$$

which quantifies the ignorance (on average) about the value of X given Y is known, we can rewrite Eq. (1) as

$$\mathcal{I}(X:Y) = H(X) - H(X|Y). \tag{3}$$

In order to generalize the above equations to the quantum domain, we replace classical probability distributions by density matrices. Denoting by ρ the density matrix of a composite system AB and by ρ^A and ρ^B, the density matrices of parts A and B, respectively, the quantum mutual information can be defined as

$$I(\rho^A:\rho^B) = S(\rho^A) - S(\rho^A|\rho^B), \tag{4}$$

where $S(\rho^A)=-\mathrm{Tr}\,\rho^A \log \rho^A$ is the von Neumann entropy for subsystem A and

$$S(\rho^A|\rho^B) = S(\rho) - S(\rho^B) \tag{5}$$

is a quantum generalization of the conditional entropy for A and B. A remarkable observation realized in Ref. [17] is that the conditional entropy can be introduced by a different approach which, although classically equivalent to Eq. (2), yields a result in the quantum case that differs from Eq. (5). Indeed, let us consider a measurement performed locally only on part B. This measurement can be described by a set of projectors $\{B_k\}$. The state of the quantum system conditioned on the measurement of the outcome labeled by k becomes

$$\rho_k = \frac{1}{p_k}(I \otimes B_k)\rho(I \otimes B_k), \tag{6}$$

where $p_k=\mathrm{Tr}[(I\otimes B_k)\rho(I\otimes B_k)]$ denotes the probability of obtaining the outcome k, and I denotes the identity operator for the subsystem A. The conditional density operator given by Eq. (6) allows for the following alternative definition of the quantum conditional entropy:

$$S(\rho|\{B_k\}) = \sum_k p_k S(\rho_k). \tag{7}$$

Therefore, following Eq. (3), the quantum mutual information can also be alternatively defined by

$$J(\rho:\{B_k\}) = S(\rho^A) - S(\rho|\{B_k\}). \tag{8}$$

Equations (4) and (8) are classically equivalent but they are different in the quantum case. The difference between them is due to quantum effects on the correlation between parts A and B and provides a measure for the quantumness of the correlation, which has been called quantum discord [17]. In fact, following Refs. [17,22], we can define the classical correlation between parts A and B as

$$C(\rho) = \max_{\{B_k\}} J(\rho:\{B_k\}), \tag{9}$$

with the quantum correlation accounted by the quantum discord, which is then given by

$$Q(\rho) = I(\rho^A:\rho^B) - C(\rho). \tag{10}$$

III. PAIRWISE CORRELATIONS FOR Z_2-SYMMETRIC QUANTUM SPIN LATTICES

We will consider here an interacting pair of spins-1/2 in a spin lattice, which is governed by a Hamiltonian H that is both real and exhibits Z_2 symmetry, i.e., invariance under π rotation around a given spin axis. By taking this spin axis as the z direction, this implies the commutation of H with the parity operator $\otimes_{i=1}^N \sigma_i^3$, where N denotes the total number of spins and σ_i^3 is the Pauli operator along the z axis at site i. Note that a number of spin models are enclosed within these requirements as, for instance, the XXZ spin chain and the transverse field Ising model. Disregarding spontaneous symmetry breaking (see, e.g., Refs. [23–25], for a treatment of spontaneously broken ground states), the two-spin reduced density matrix at sites labeled by i and j in the basis $\{|\uparrow\uparrow\rangle,|\uparrow\downarrow\rangle,|\downarrow\uparrow\rangle,|\downarrow\downarrow\rangle\}$, with $|\uparrow\rangle$ and $|\downarrow\rangle$ denoting the eigenstates of σ^3, will be given by

$$\rho = \begin{pmatrix} a & 0 & 0 & f \\ 0 & b_1 & z & 0 \\ 0 & z & b_2 & 0 \\ f & 0 & 0 & d \end{pmatrix}. \tag{11}$$

In terms of spin-correlation functions, these elements can be written as

$$a = \frac{1}{4}(1 + G_z^i + G_z^j + G_{zz}^{ij}),$$

$$b_1 = \frac{1}{4}(1 + G_z^i - G_z^j - G_{zz}^{ij}),$$

$$b_2 = \frac{1}{4}(1 - G_z^i + G_z^j - G_{zz}^{ij}),$$

$$d = \frac{1}{4}(1 - G_z^i - G_z^j + G_{zz}^{ij}),$$

$$z = \frac{1}{4}(G_{xx}^{ij} + G_{yy}^{ij}),$$

$$f = \frac{1}{4}(G_{xx}^{ij} - G_{yy}^{ij}), \tag{12}$$

where $G_z^k=\langle\sigma_z^k\rangle$ $(k=i,j)$ is the magnetization density at site k and $G_{\alpha\beta}^{ij}=\langle\sigma_\alpha^i\sigma_\beta^j\rangle$ $(\alpha,\beta=x,y,z)$ denote two-point spin-spin

functions at sites i and j, with the expectation value taken over the quantum state of the system. Note that in case of translation invariance, we will have that $G_z^k = G_z^{k'}(\forall k,k')$ and, therefore, $b_1 = b_2$. Moreover, observe also that the density operator given in Eq. (11) can be decomposed as

$$\rho = \frac{1}{4}\left[I \otimes I + \sum_{i=1}^{3} (c_i \sigma^i \otimes \sigma^i) + c_4 I \otimes \sigma^3 + c_5 \sigma^3 \otimes I \right], \quad (13)$$

with

$$c_1 = 2z + 2f,$$

$$c_2 = 2z - 2f,$$

$$c_3 = a + d - b_1 - b_2,$$

$$c_4 = a - d - b_1 + b_2,$$

$$c_5 = a - d + b_1 - b_2. \quad (14)$$

In particular, for translation invariant systems, we have that $c_4 = c_5$. In order to determine classical and quantum correlations, we first evaluate the mutual information as given by Eq. (4). The eigenvalues of ρ read as

$$\lambda_0 = \frac{1}{4}[(1 + c_3) + \sqrt{(c_4 + c_5)^2 + (c_1 - c_2)^2}],$$

$$\lambda_1 = \frac{1}{4}[(1 + c_3) - \sqrt{(c_4 + c_5)^2 + (c_1 - c_2)^2}],$$

$$\lambda_2 = \frac{1}{4}[(1 - c_3) + \sqrt{(c_4 - c_5)^2 + (c_1 + c_2)^2}],$$

$$\lambda_3 = \frac{1}{4}[(1 - c_3) - \sqrt{(c_4 - c_5)^2 + (c_1 + c_2)^2}]. \quad (15)$$

Therefore, the mutual information is given by

$$I(\rho) = S(\rho^A) + S(\rho^B) + \sum_{\alpha=0}^{3} \lambda_\alpha \log \lambda_\alpha, \quad (16)$$

where

$$S(\rho^A) = -(r_1^A \log r_1^A + r_2^A \log r_2^A),$$

$$S(\rho^B) = -(r_1^B \log r_1^B + r_2^B \log r_2^B), \quad (17)$$

with $r_1^A = (1+c_5)/2$, $r_2^A = (1-c_5)/2$, $r_1^B = (1+c_4)/2$, and $r_2^B = (1-c_4)/2$. Classical correlations can be obtained by following a procedure that is similar to those of Refs. [18,21], but applying it now for the case of the general density matrix given by Eq. (11). We first introduce a set of projectors for a local measurement on part B given by $\{B_k = V\Pi_k V^\dagger\}$, where $\{\Pi_k = |k\rangle\langle k| : k = 0,1\}$ is the set of projectors on the computational basis ($|0\rangle \equiv |\uparrow\rangle$ and $|1\rangle \equiv |\downarrow\rangle$) and $V \in U(2)$. Note that the projectors B_k represent therefore an arbitrary local measurement on B. We parametrize V as

$$V = \begin{pmatrix} \cos\frac{\theta}{2} & \sin\frac{\theta}{2} e^{-i\phi} \\ \sin\frac{\theta}{2} e^{i\phi} & -\cos\frac{\theta}{2} \end{pmatrix}, \quad (18)$$

where $0 \le \theta \le \pi$ and $0 \le \phi < 2\pi$. Note that θ and ϕ can be interpreted as the azimuthal and polar angles, respectively, of a qubit over the Bloch sphere. By using Eq. (6) and the equation $\Pi_k \sigma^i \Pi_k = \delta_{i3}(-1)^k \Pi_k$, with δ_{i3} denoting the Kronecker symbol, we can show that the state of the system after measurement $\{B_k\}$ will change to one of the states

$$\rho_0 = \frac{1}{2}\left(I + \sum_{j=1}^{3} q_{0j} \sigma^j \right) \otimes (V\Pi_0 V^\dagger), \quad (19)$$

$$\rho_1 = \frac{1}{2}\left(I + \sum_{j=1}^{3} q_{1j} \sigma^j \right) \otimes (V\Pi_1 V^\dagger), \quad (20)$$

where

$$q_{k1} = (-1)^k c_1 \left[\frac{w_1}{1 + (-1)^k c_4 w_3} \right],$$

$$q_{k2} = (-1)^k c_2 \left[\frac{w_2}{1 + (-1)^k c_4 w_3} \right],$$

$$q_{k3} = (-1)^k \left[\frac{c_3 w_3 + (-1)^k c_5}{1 + (-1)^k c_4 w_3} \right], \quad (21)$$

with $k = 0,1$ and

$$w_1 = \sin\theta \cos\phi,$$

$$w_2 = \sin\theta \sin\phi,$$

$$w_3 = \cos\theta. \quad (22)$$

Then, by evaluating von Neumann entropy from Eqs. (19) and (20) and using that $S(V\Pi_k V^\dagger) = 0$, we obtain

$$S(\rho_k) = -\frac{(1+\theta_k)}{2}\log\frac{(1+\theta_k)}{2} - \frac{(1-\theta_k)}{2}\log\frac{(1-\theta_k)}{2}, \quad (23)$$

with

$$\theta_k = \sqrt{\sum_{j=1}^{3} q_{kj}^2}. \quad (24)$$

Therefore, the classical correlation for the spin pair at sites i and j will be given by

$$C(\rho) = \max_{\{B_k\}} \left[S(\rho^A) - \frac{(S_0 + S_1)}{2} - c_4 w_3 \frac{(S_0 - S_1)}{2} \right], \quad (25)$$

where $S_k = S(\rho_k)$. For some cases, the maximization in Eq. (25) can be worked out and an expression purely in terms of the spin-correlation functions can be obtained (e.g., the XXZ and Ising chains below). In general, however, $C(\rho)$ has to be numerically evaluated by optimizing over the angles θ and ϕ. Once classical correlation is obtained, the insertion of

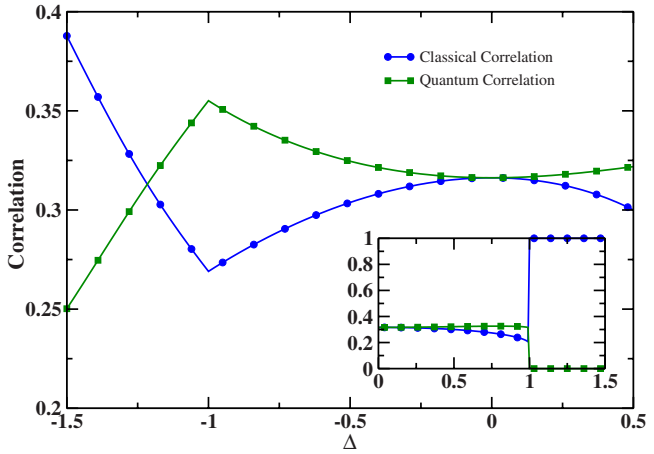

FIG. 1. (Color online) Quantum and classical correlations for nearest-neighbor spins in the *XXZ* chain for $L\to\infty$.

Eqs. (16) and (25) into Eq. (10) can be used to determine the quantum discord.

IV. *XXZ* SPIN CHAIN

Let us illustrate the discussion of classical and quantum correlations between two spins by considering the *XXZ* spin chain, whose Hamiltonian is given by

$$H_{XXZ}=-\frac{J}{2}\sum_{i=1}^{L}(\sigma_i^x\sigma_{i+1}^x+\sigma_i^y\sigma_{i+1}^y+\Delta\sigma_i^z\sigma_{i+1}^z), \tag{26}$$

where periodic boundary conditions are assumed, ensuring therefore translation symmetry. We will set the energy scale such that $J=1$ and will be interested in a nearest-neighbor spin pair at sites i and $i+1$. Concerning its symmetries, the *XXZ* chain exhibits $U(1)$ invariance, namely, $[H,\Sigma_i\sigma_z^i]=0$, which provides a stronger constraint over the elements of the density matrix than the Z_2 symmetry. Indeed, $U(1)$ invariance ensures that the element f of the reduced density matrix given by Eq. (11) vanishes. Moreover, the ground state has magnetization density $G_z^k=\langle\sigma_z^k\rangle=0$ $(\forall k)$, which implies that

$$a=d=\frac{1}{4}(1+G_{zz}),$$

$$b_1=b_2=\frac{1}{4}(1-G_{zz}),$$

$$z=\frac{1}{4}(G_{xx}+G_{yy}),$$

$$f=0, \tag{27}$$

where, due to translation invariance, we write $G_{\alpha\beta}=\langle\sigma_\alpha^i\sigma_\beta^{i+1}\rangle$ $(\forall i)$. Due to the fact that $a=d$, we will have that $c_4=c_5=0$, which considerably simplifies the computation of classical and quantum correlations. Moreover, we will have that $c_1=c_2=2z$ and $c_3=4a-1$. Then, the maximization procedure in Eq. (25) can be analytically worked out [18], yielding

$$C(\rho)=\frac{(1-c)}{2}\log(1-c)+\frac{(1+c)}{2}\log(1+c), \tag{28}$$

with $c=\max(|c_1|,|c_2|,|c_3|)$. For the mutual information $I(\rho)$, we obtain

$$I(\rho)=2+\sum_{i=0}^{3}\lambda_i\log\lambda_i, \tag{29}$$

where

$$\lambda_0=\frac{1}{4}(1-c_1-c_2-c_3),$$

$$\lambda_1=\frac{1}{4}(1-c_1+c_2+c_3),$$

$$\lambda_2=\frac{1}{4}(1+c_1-c_2+c_3),$$

$$\lambda_3=\frac{1}{4}(1+c_1+c_2-c_3). \tag{30}$$

In order to compute $C(\rho)$ and $Q(\rho)$, we write c_1, c_2, and c_3 in terms of the ground-state energy density. By using the Hellmann-Feynman theorem [26,27] for the *XXZ* Hamiltonian (26), we obtain

$$c_1=c_2=\frac{1}{2}(G_{xx}+G_{yy})=\Delta\frac{\partial\varepsilon_{xxz}}{\partial\Delta}-\varepsilon_{xxz},$$

$$c_3=G_{zz}=-2\frac{\partial\varepsilon_{xxz}}{\partial\Delta}, \tag{31}$$

where ε_{xxz} is the ground-state energy density

$$\varepsilon_{xxz}=\frac{\langle\psi_0|H_{XXZ}|\psi_0\rangle}{L}=-\frac{1}{2}(G_{xx}+G_{yy}+\Delta G_{zz}), \tag{32}$$

with $|\psi_0\rangle$ denoting the ground state of H_{XXZ}. Equations (31) and (32) hold for a chain with an arbitrary number of sites, allowing the discussion of correlations either for finite or infinite chains. Indeed, the ground-state energy as well as its derivatives can be exactly determined by Bethe ansatz technique [28], which allows us to obtain the correlation functions c_1, c_2, and c_3. In Fig. 1, we plot classical and quantum correlations between nearest-neighbor pairs for an infinite *XXZ* spin chain.

Note that in the classical Ising limit $\Delta\to\infty$, we have a fully polarized ferromagnet. The ground state is then a doublet given by the vectors $|\uparrow\uparrow\cdots\uparrow\rangle$ and $|\downarrow\downarrow\cdots\downarrow\rangle$, yielding the mixed state

$$\rho=\frac{1}{2}|\uparrow\uparrow\cdots\uparrow\rangle\langle\uparrow\uparrow\cdots\uparrow|+\frac{1}{2}|\downarrow\downarrow\cdots\downarrow\rangle\langle\downarrow\downarrow\cdots\downarrow|. \tag{33}$$

Indeed, this is simply a classical probability mixing, with $C(\rho)=I(\rho)=1$ and $Q(\rho)=0$. The same applies for the antiferromagnetic Ising limit $\Delta\to-\infty$, where a doubly degenerate ground state arises. Moreover, observe that the classical

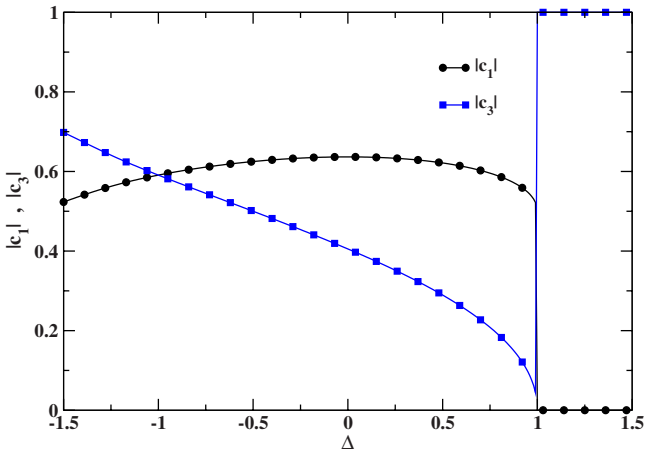

FIG. 2. (Color online) Values of the parameters $|c_1|=|c_2|$ and $|c_3|$ as a function of Δ. The parameter $|c_3|$ governs the correlations for $\Delta<-1$, while $|c_1|=|c_2|$ is dominant in the gapless disordered phase $-1<\Delta<1$. In the ferromagnetic phase, $|c_1|=|c_2|=0$ and $|c_3|=1$, which implies the fixed value $C(\rho)=1$ and $Q(\rho)=0$ for any $\Delta>1$.

(quantum) correlation is a minimum (maximum) at the infinite-order QCP $\Delta=-1$. On the other hand, both correlations are discontinuous at the first-order QCP $\Delta=1$. This is indeed in agreement with the usual behavior of entanglement both at infinite and first-order QPTs. For an infinite-order QCP, entanglement commonly displays a maximum at the QCP [29–31], while for a first-order QCP, entanglement usually exhibits a jump at the QCP [32,33]. Nevertheless, we note that in the specific case of the ferromagnetic QCP $\Delta=1$ and for pairwise entanglement measures, such as concurrence [34] and negativity [35], no jump is detected, being hidden by the operation max [36]. It is interesting to observe the behavior of the functions $|c_1|=|c_2|$ and $|c_3|$ that govern the classical and quantum correlations. For $\Delta<-1$, we have that $|c_1|=|c_2|<|c_3|$, which means that the classical correlation is governed by $|c_3|$. For $-1<\Delta<1$, we have that $|c_1|=|c_2|>|c_3|$, with the crossing occurring exactly at the infinite-order QCP. Therefore, the correlations are governed by different parameters in different phases. For $\Delta\geq 1$, we obtain $|c_1|=|c_2|=0$ and $|c_3|=1$, which implies that $C(\rho)=1$ and $Q(\rho)=0$. These results are shown in Fig. 2.

V. TRANSVERSE FIELD ISING MODEL

Let us consider now the Ising chain in a transverse magnetic field, whose Hamiltonian is given by

$$H_I=-J\sum_{i=1}^{L}(\sigma_i^x\sigma_{i+1}^x+g\sigma_i^z), \tag{34}$$

with periodic boundary conditions assumed, namely, $\sigma_{L+1}^x=\sigma_1^x$. As before, we will set the energy scale such that $J=1$ and will be interested in a nearest-neighbor spin pair at sites i and $i+1$. This Hamiltonian is Z_2 symmetric and can be exactly diagonalized by mapping it to a spinless free fermion model with single orbitals. This is implemented through the Jordan-Wigner transformation,

$$\sigma_i^z=1-2c_i^\dagger c_i,$$

$$\sigma_i^x=-\prod_{j<i}(1-2c_j^\dagger c_j)(c_i+c_i^\dagger), \tag{35}$$

where $c_i^\dagger$ and c_i are the creation and annihilation fermion operators at site i, respectively. By rewriting Eq. (34) in terms of $c_i^\dagger$ and c_i, we obtain

$$H_I=-J\sum_{i=1}^{L}(c_i^\dagger c_{i+1}+c_{i+1}^\dagger c_i+c_i^\dagger c_{i+1}^\dagger+c_i c_{i+1})$$

$$-Jg\sum_{i=1}^{L}(1-2c_i^\dagger c_i). \tag{36}$$

In order to diagonalize H_I, we consider fermions in momentum space,

$$c_k=\frac{1}{\sqrt{L}}\sum_{j=1}^{L}c_j e^{-ikr_j},$$

$$c_k^\dagger=\frac{1}{\sqrt{L}}\sum_{j=1}^{L}c_j^\dagger e^{ikr_j}, \tag{37}$$

where $c_k^\dagger$ and c_k are creation and annihilation fermion operators with momentum k, respectively, and r_j is the fermion position at site j. The wave vectors $\vec{k}$ satisfy the relation $ka=2\pi q/L$, where a denotes the distance between two nearest-neighbor sites and $q=-M,-M+1,\ldots,M-1,M$, with $M=(L-1)/2$ and L taken, for simplicity, as an even number. Then, by inverting Eq. (37) and inserting the result in Eq. (36), we obtain

$$H_I=J\sum_k[2(g-\cos ka)c_k^\dagger c_k+i\sin ka(c_{-k}^\dagger c_k^\dagger+c_{-k}c_k)-g]. \tag{38}$$

Diagonalization is then obtained by eliminating the terms $c_{-k}^\dagger c_k^\dagger$ and $c_{-k}c_k$ from the Hamiltonian given by Eq. (38), which do not conserve the particle number. This is indeed achieved through the Bogoliubov transformation in which new fermion operators γ_k and $\gamma_k^\dagger$ are introduced as linear combination of c_k and $c_k^\dagger$,

$$\gamma_k=u_k c_k-iv_k c_{-k}^\dagger,$$

$$\gamma_k^\dagger=u_k c_k^\dagger+iv_k c_{-k}, \tag{39}$$

where u_k and v_k are real numbers parametrized by $u_k=\sin\theta_k/2$ and $v_k=\cos\frac{\theta_k}{2}$. This parametrization naturally arises as a consequence of the fermionic algebra $\{\gamma_k,\gamma_{k'}^\dagger\}=\delta_{kk'}$, $\{\gamma_k^\dagger,\gamma_{k'}^\dagger\}=\{\gamma_k,\gamma_{k'}\}=0$, with $\delta_{kk'}$ standing for the Kronecker delta symbol. Moreover, to recast the Hamiltonian in a diagonal form we define θ_k by demanding that $\tan\theta_k=\sin ka/(g-\cos ka)$. Therefore, by expressing H_I in terms of Bogoliubov fermions and by imposing the trace invariance of the Hamiltonian, Eq. (38) becomes

$$H_I = \sum_k \varepsilon_k \left(\gamma_k^\dagger \gamma_k - \frac{1}{2} \right), \tag{40}$$

with $\varepsilon_k = 2J\sqrt{1+g^2-2g\cos ka}$. Hamiltonian (40) is diagonal, with ground state given by the γ-fermion vacuum. The procedure above also applies for the evaluation of the matrix elements of the reduced density operator given by Eq. (12), which amounts for the computation of the magnetization density G_z and the two-point functions $G_{\alpha\beta}$. This can be achieved by using that $G_{zz} = G_z^2 - G_{xx}G_{yy}$ [37] and by expressing the remaining correlation functions as

$$G_{xx} = \frac{2}{L}\sum_{q=-M}^{M} \left[\cos\left(\frac{2\pi q}{L}\right) v_q^2 + \sin\left(\frac{2\pi q}{L}\right) u_q v_q \right],$$

$$G_{yy} = \frac{2}{L}\sum_{q=-M}^{M} \left[\cos\left(\frac{2\pi q}{L}\right) v_q^2 - \sin\left(\frac{2\pi q}{L}\right) u_q v_q \right],$$

$$G_z = \frac{1}{L}\sum_{q=-M}^{M} (1 - 2v_q^2), \tag{41}$$

where

$$u_q v_q = \frac{1}{2} \frac{\sin\left(\frac{2\pi q}{L}\right)}{\sqrt{1+g^2-2g\cos\left(\frac{2\pi q}{L}\right)}},$$

$$v_q^2 = \frac{1}{2}\left[1 - \frac{\left[g - \cos\left(\frac{2\pi q}{L}\right) \right]}{\sqrt{1+g^2-2g\cos\left(\frac{2\pi q}{L}\right)}} \right]. \tag{42}$$

Hence, we exactly determine the two-spin reduced density matrix. Classical and quantum correlations can then be directly obtained from Eqs. (9) and (10). By numerically computing the classical correlation in Eq. (25) for nearest-neighbor spin pairs at sites i and $i+1$, we can show that the maximization is achieved for any g by the choice $\theta = \pi/2$ and $\phi = 0$. Then, the measurement that maximizes $J(\rho:\{B_k\})$ is given by $\{|+\rangle\langle+|, |-\rangle\langle-|\}$, with $|+\rangle$ and $|-\rangle$ denoting the up and down spins in the x direction, namely, $|\pm\rangle = (|\uparrow\rangle \pm |\uparrow\rangle)/\sqrt{2}$. This numerical observation implies that $w_1 = 1$, $w_2 = w_3 = 0$. Therefore, Eq. (25) is ruled by the spin functions $c_1 = G_{xx}^{i,i+1}$ and $c_4 = c_5 = G_z^i$, i.e.,

$$C(\rho) = H_{bin}(p_1) - H_{bin}(p_2), \tag{43}$$

where H_{bin} is the binary entropy,

$$H_{bin}(p) = -p\log p - (1-p)\log(1-p), \tag{44}$$

and

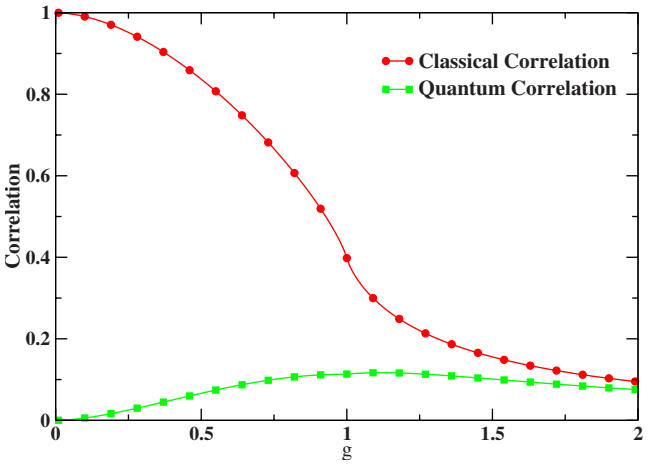

FIG. 3. (Color online) Classical and quantum correlations for nearest-neighbor spins in the transverse field Ising model for a chain with 1024 sites.

$$p_1 = \frac{1}{2}(1 + G_z^i),$$

$$p_2 = \frac{1}{2}\left[1 + \sqrt{(G_{xx}^{i,i+1})^2 + (G_z^i)^2}\right]. \tag{45}$$

We plot $C(\rho)$ and $Q(\rho)$ in Fig. 3 for a chain with 1024 sites. Note that for $g=0$, the system is a classical Ising chain, whose ground state is a doublet given by the vectors $|{+}{+}\cdots{+}\rangle$ and $|{-}{-}\cdots{-}\rangle$. Therefore, the system is in the mixed state

$$\rho = \frac{1}{2}|{+}\,{+}\cdots{+}\rangle\langle{+}\,{+}\cdots{+}| + \frac{1}{2}|{-}\,{-}\cdots{-}\rangle\langle{-}\,{-}\cdots{-}|, \tag{46}$$

with $C(\rho) = I(\rho) = 1$ and $Q(\rho) = 0$. On the other hand, in the limit $g \to \infty$ the system is a paramagnet (vanishing magnetization in the x direction), with all spins in state $|\uparrow\rangle$. Therefore, the system will be described by the density operator,

$$\rho = |\uparrow\uparrow\cdots\uparrow\rangle\langle\uparrow\uparrow\cdots\uparrow|, \tag{47}$$

which is a pure separable state, containing neither classical nor quantum correlations.

The QPT from ferromagnetic to paramagnetic state is a second-order QPT and occurs at $g=1$. Signatures of this QPT can be found out by looking at the derivatives of either classical or quantum correlations. Indeed, the QPT can be identified as a pronounced minimum of the first derivative of the classical correlation, which is exhibited in Fig. 4. Note that the minimum logarithmically diverges at $g=1$ as the thermodynamic limit is approached (see inset of Fig. 4). In the case of quantum correlations, its first derivative shows an inflexion point around $g=1$, as displayed in Fig. 5. Indeed, by looking at its second derivative in Fig. 6, the QPT is identified by a pronounced maximum, which shows quadratic logarithmic divergence at $g=1$ as the thermodynamic limit is approached (see inset of Fig. 6).

The behavior of the quantum discord is therefore rather different from the entanglement behavior, whose first deriva-

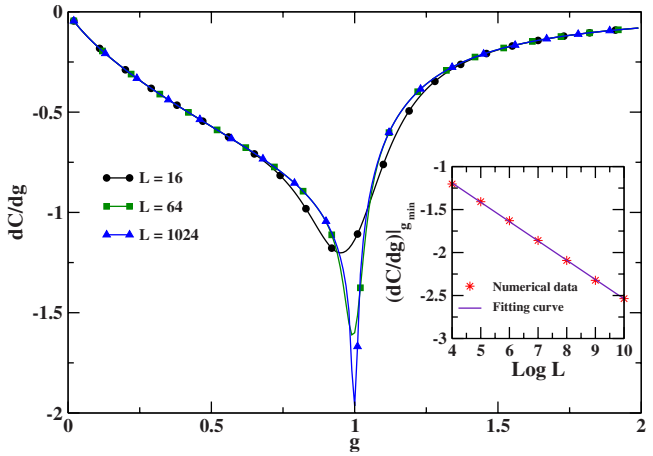

FIG. 4. (Color online) First derivative of the classical correlation for nearest-neighbor spins with respect to g in the transverse field Ising chain for different lattice sizes L. The derivative of C has a pronounced minimum at g_{min}, which tends to the QCP $g=1$ as $L\to\infty$. Inset: dC/dg taken at g_{min} exhibits a logarithmic divergence fitted by $(dC/dg)|_{g_{min}}=-0.29161-0.22471\log L$.

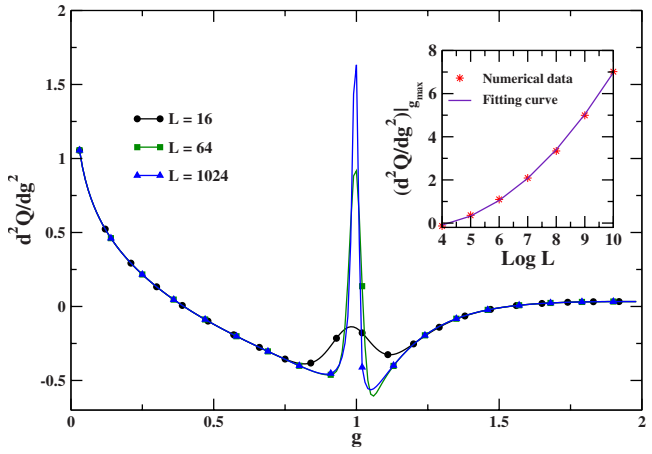

FIG. 6. (Color online) Second derivative of the quantum correlations for nearest-neighbor spins with respect to g in the transverse field Ising chain for different lattice sizes L. Observe that the second derivative of Q has a pronounced maximum at g_{max}, which tends to the QCP $g=1$ as $L\to\infty$. Inset: d^2C/dg^2 taken at g_{max} exhibits a quadratic logarithmic divergence fitted by $(d^2Q/dg^2)|_{g_{max}}=1.268-0.94712\log L+0.15176\log^2 L$.

tive is already divergent at the QCP. Remarkably, the scaling of pairwise entanglement derivative in this case (see, e.g., Refs. [4,5]) is much closer to the scaling of the classical correlation derivative (as given by Fig. 4) than that of the quantum correlation derivative (as given by Fig. 5). As in the case of the *XXZ* model, it is interesting to observe that the spin functions $c_1=G_{xx}^{i,i+1}$ and $c_4=c_5=G_z^i$, which govern the correlations in the Ising chain [see Eqs. (43)–(45)], exhibit a crossing at the QCP. This is shown in Fig. 7 for a chain with 1024 sites.

VI. LMG MODEL

The discussion of correlations above can also be applied in collective systems. As an illustration, we will consider here the LMG model [38], which describes a two-level Fermi system $\{|+\rangle,|-\rangle\}$, with each level having degeneracy Ω. The Hamiltonian for LMG model is given by

$$H=\lambda\sum_{m=1}^{\Omega}\frac{1}{2}(c_{+m}^{\dagger}c_{+m}-c_{-m}^{\dagger}c_{-m})-\frac{1}{2N}\sum_{m,n=1}^{\Omega}(c_{+m}^{\dagger}c_{-m}c_{+n}^{\dagger}c_{-n}+c_{-n}^{\dagger}c_{+n}c_{-m}^{\dagger}c_{+m}). \quad (48)$$

The operators $c_{+m}^{\dagger}$ and $c_{-m}^{\dagger}$ create a particle in the upper and lower levels, respectively. This Hamiltonian can be taken as describing an effective model for many-body systems, with one level just below the Fermi level and the other level just above, with the level below being filled with Ω particles [39]. Alternatively, the LMG model can be seen as a one-

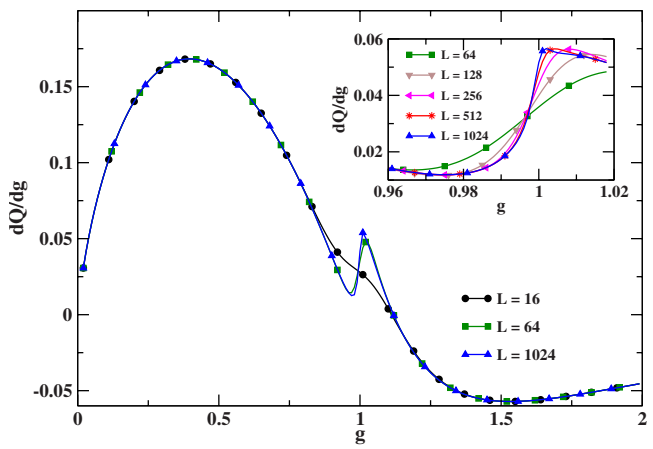

FIG. 5. (Color online) First derivative of the quantum correlation for nearest-neighbor spins with respect to g in the transverse field Ising chain for different lattice sizes L. Inset: dQ/dg presents an inflexion point that tends to the QCP $g=1$ as $L\to\infty$.

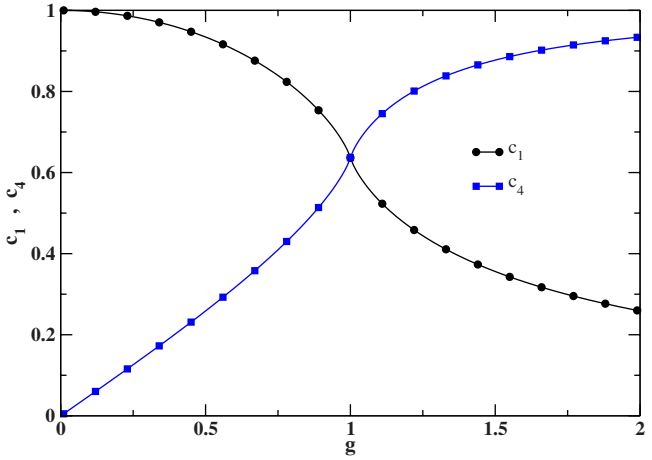

FIG. 7. (Color online) Spin functions $c_1=G_{xx}^{i,i+1}$ and $c_4=G_z^i$ as a function of g. These functions govern the behavior of correlations, exhibiting a crossing exactly at the QCP. The plot is for a chain with $L=1024$ sites.

dimensional ring of spin-1/2 particles with an infinite range interaction between pairs. Indeed, the Hamiltonian can be rewritten as

$$H = \lambda S_z - \frac{1}{N}(S_x^2 - S_y^2), \tag{49}$$

where $S_z = \Sigma_{m=1}^{N} \frac{1}{2}(c_{+m}^{\dagger} c_{+m} - c_{-m}^{\dagger} c_{-m})$ and $S_x + iS_y = \Sigma_{m=1}^{N} c_{+m}^{\dagger} c_{-m}$ [39]. The system undergoes a second-order QPT at $\lambda = 1$. As $\Omega \to \infty$, the ground state, as given by the HF approach, reads as

$$|\mathrm{HF}\rangle = \prod_{m=1}^{\omega} a_{0m}^{\dagger} |-\rangle, \tag{50}$$

where we have introduced new levels labeled by 0 and 1 governed by the operators

$$a_{0m}^{\dagger} = \cos\alpha c_{-m}^{\dagger} + \sin\alpha c_{+m}^{\dagger},$$

$$a_{1m}^{\dagger} = -\sin\alpha c_{-m}^{\dagger} + \cos\alpha c_{+m}^{\dagger}. \tag{51}$$

In Eq. (51), α is a variational parameter to be adjusted in order to minimize energy, which is achieved according to the choice

$$\lambda < 1 \Rightarrow \cos 2\alpha = \lambda,$$

$$\lambda \geq 1 \Rightarrow \alpha = 0. \tag{52}$$

Despite being an approximation, the HF ground state provides the exact description of the critical point (for recent discussions of the exact spectrum of the LMG model, see Refs. [40,41]). The pairwise density operator for general modes $i \equiv (+m)$ and $j \equiv (-n)$ is given by

$$\rho_{i,j} = \begin{pmatrix} \langle M_i M_j \rangle & 0 & 0 & 0 \\ 0 & \langle M_i N_j \rangle & \langle c_i^{\dagger} c_j \rangle & 0 \\ 0 & \langle c_j^{\dagger} c_i \rangle & \langle N_i M_j \rangle & 0 \\ 0 & 0 & 0 & \langle N_i N_j \rangle \end{pmatrix}, \tag{53}$$

where $M_k = 1 - N_k$ and $N_k = c_k^{\dagger} c_k$, with $k = i, j$. By evaluating the matrix elements of ρ for the HF ground state, we obtain

$$\langle M_{+m} M_{-n} \rangle = \sin^2\alpha \cos^2\alpha (1 - \delta_{mn}),$$

$$\langle M_{+m} N_{-n} \rangle = \cos^2\alpha \delta_{mn} + \cos^4\alpha (1 - \delta_{mn}),$$

$$\langle N_{+m} M_{-n} \rangle = \sin^2\alpha \delta_{mn} + \sin^4\alpha (1 - \delta_{mn}),$$

$$\langle N_{+m} N_{-n} \rangle = \sin^2\alpha \cos^2\alpha (1 - \delta_{mn}),$$

$$\langle c_{+m}^{\dagger} c_{-n} \rangle = \sin\alpha \cos\alpha \delta_{mn},$$

$$\langle c_{-n}^{\dagger} c_{+m} \rangle = \sin\alpha \cos\alpha \delta_{mn}. \tag{54}$$

Note that Eq. (53) displays Z_2 symmetry and, therefore, classical and quantum correlations can be computed by using Eq. (25). Note also that for $m \neq n$, the density matrix is diagonal and the state is completely pairwise uncorrelated. On the other hand, for $m = n$, there is an equal amount of classical and quantum correlations between the modes. These correlations vanish for $\lambda > 1$, which is the fully polarized state. The result is plotted in Fig. 8. We can then observe that the derivatives of both classical correlation and quantum discord exhibit a signature of the QPT (see the inset of Fig. 8). These signatures are in agreement with the characterizations in terms of entanglement [42,43] and Fisher information [44].

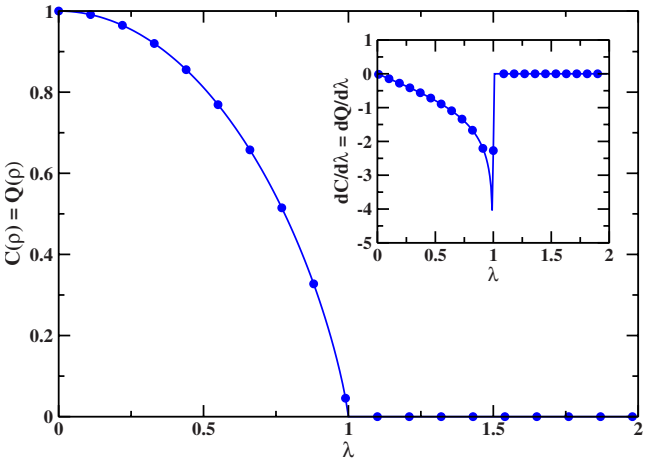

FIG. 8. (Color online) Classical and quantum correlations between modes $(+m)$ and $(-m)$ in the HF ground state of the Lipkin model. Inset: derivative of correlations is nonanalytic at $\lambda = 1$.

VII. CONCLUSION

In conclusion, we have investigated the behavior of pairwise correlations in general Z_2 symmetric systems, splitting up their classical and quantum contributions. This allowed for the treatment of spin systems such as the *XXZ* model and the transverse field Ising chain, where the maximization required for the evaluation of the correlations has been analytically worked out. Moreover, we have identified the spin functions that govern the correlations and also discussed their behavior for finite-size chains. As a further application, we have used our approach to investigate the case of a collective model given by the LMG Hamiltonian.

As it was shown, both classical correlation and quantum discord display signatures of the critical behavior of the system for the cases of first-order, second-order, and infinite-order QPTs. For first-order QPTs, as illustrated by the ferromagnetic point of the *XXZ* spin chain, we found that both classical correlation and quantum discord display a jump at the critical point, which closely resembles the behavior of entanglement. For second-order QPTs, although both kind of correlations exhibit signatures of the QPTs, the derivatives of the quantum discord show a scaling that is rather different from the entanglement behavior in the transverse field Ising model (see, e.g., Refs. [4,5]). It is remarkable that for this model, the first derivative of pairwise entanglement with respect to the parameter that drives the QPT exhibits a scaling that is much closer to the scaling of the first derivative of the *classical* correlation. For infinite-order QPTs, as given by the antiferromagnetic point of the *XXZ* spin chain, classical correlation is a minimum at the QCP while quantum discord is a

maximum. Whether or not this might be a general feature of infinite-order QPTs is still under analysis.

Further investigations including correlations between blocks of particles and the effect of temperature may be interesting to establish a precise comparison between (classical and quantum) correlations and entanglement at QPTs. Moreover, dynamics in open quantum systems [45–47] may also provide an interesting scenario for the discussion of the properties of the correlations and its implications for phase transitions. Such topics are left for a future research.

ACKNOWLEDGMENTS

This work was supported by the Brazilian agencies MCT/CNPq and FAPERJ.

[1] S. Sachdev, *Quantum Phase Transitions* (Cambridge University Press, Cambridge, England, 2001).
[2] M. A. Continentino, *Quantum Scaling in Many-Body Systems* (World Scientific, Singapore, 2001).
[3] L. Amico, R. Fazio, A. Osterloh, and V. Vedral, Rev. Mod. Phys. **80**, 517 (2008).
[4] A. Osterloh, L. Amico, G. Falci, and R. Fazio, Nature (London) **416**, 608 (2002).
[5] L.-A. Wu, M. S. Sarandy, and D. A. Lidar, Phys. Rev. Lett. **93**, 250404 (2004).
[6] G. Vidal, J. I. Latorre, E. Rico, and A. Kitaev, Phys. Rev. Lett. **90**, 227902 (2003).
[7] V. E. Korepin, Phys. Rev. Lett. **92**, 096402 (2004).
[8] P. Calabrese and J. Cardy, J. Stat. Mech.: Theory Exp. (2004) P06002.
[9] G. Refael and J. E. Moore, Phys. Rev. Lett. **93**, 260602 (2004).
[10] A. Saguia, M. S. Sarandy, B. Boechat, and M. A. Continentino, Phys. Rev. A **75**, 052329 (2007).
[11] Y.-C. Lin, F. Iglói, and H. Rieger, Phys. Rev. Lett. **99**, 147202 (2007).
[12] K. Le Hur, P. Doucet-Beaupré, and W. Hofstetter, Phys. Rev. Lett. **99**, 126801 (2007).
[13] M. B. Plenio, J. Eisert, J. Dreißig, and M. Cramer, Phys. Rev. Lett. **94**, 060503 (2005).
[14] M. M. Wolf, Phys. Rev. Lett. **96**, 010404 (2006).
[15] R. Yu, H. Saleur, and S. Haas, Phys. Rev. B **77**, 140402(R) (2008).
[16] M. M. Wolf, F. Verstraete, M. B. Hastings, and J. I. Cirac, Phys. Rev. Lett. **100**, 070502 (2008).
[17] H. Ollivier and W. H. Zurek, Phys. Rev. Lett. **88**, 017901 (2001).
[18] S. Luo, Phys. Rev. A **77**, 042303 (2008).
[19] D. Kaszlikowski, A. Sen(De), U. Sen, V. Vedral, and A. Winter, Phys. Rev. Lett. **101**, 070502 (2008).
[20] A. Grudka, M. Horodecki, P. Horodecki, and R. Horodecki, e-print arXiv:0805.3060.
[21] R. Dillenschneider, Phys. Rev. B **78**, 224413 (2008).
[22] L. Henderson and V. Vedral, J. Phys. A **34**, 6899 (2001).
[23] O. F. Syljuåsen, Phys. Rev. A **68**, 060301(R) (2003).
[24] A. Osterloh, G. Palacios, and S. Montangero, Phys. Rev. Lett. **97**, 257201 (2006).
[25] T. R. de Oliveira, G. Rigolin, M. C. de Oliveira, and E. Miranda, Phys. Rev. A **77**, 032325 (2008).
[26] H. Hellmann, *Die Einführung in die Quantenchemie* (Deuticke, Leipzig, 1937).
[27] R. P. Feynman, Phys. Rev. **56**, 340 (1939).
[28] C. N. Yang and C. P. Yang, Phys. Rev. **150**, 321 (1966); **150**, 327 (1966).
[29] S.-J. Gu, H.-Q. Lin, and Y.-Q. Li, Phys. Rev. A **68**, 042330 (2003).
[30] S.-J. Gu, S.-S. Deng, Y.-Q. Li, and H.-Q. Lin, Phys. Rev. Lett. **93**, 086402 (2004).
[31] V. V. França and K. Capelle, Phys. Rev. A **74**, 042325 (2006).
[32] I. Bose and E. Chattopadhyay, Phys. Rev. A **66**, 062320 (2002).
[33] F. C. Alcaraz, A. Saguia, and M. S. Sarandy, Phys. Rev. A **70**, 032333 (2004).
[34] W. K. Wootters, Phys. Rev. Lett. **80**, 2245 (1998).
[35] G. Vidal and R. F. Werner, Phys. Rev. A **65**, 032314 (2002).
[36] M.-F. Yang, Phys. Rev. A **71**, 030302(R) (2005).
[37] P. Pfeuty, Ann. Phys. **57**, 79 (1970).
[38] H. J. Lipkin, N. Meshkov, and A. J. Glick, Nucl. Phys. **62**, 188 (1965).
[39] P. Ring and P. Schuck, *The Nuclear Many-Body Problem* (Springer, New York, 1980).
[40] P. Ribeiro, J. Vidal, and R. Mosseri, Phys. Rev. Lett. **99**, 050402 (2007).
[41] P. Ribeiro, J. Vidal, and R. Mosseri, Phys. Rev. E **78**, 021106 (2008).
[42] J. Vidal, G. Palacios, and R. Mosseri, Phys. Rev. A **69**, 022107 (2004).
[43] L.-A. Wu, M. S. Sarandy, D. A. Lidar, and L. J. Sham, Phys. Rev. A **74**, 052335 (2006).
[44] J. Ma and X. Wang, Phys. Rev. A **80**, 012318 (2009).
[45] A. Shabani and D. A. Lidar, Phys. Rev. Lett. **102**, 100402 (2009).
[46] T. Werlang, S. Souza, F. F. Fanchini, and C. Villas-Boas, e-print arXiv:0905.3376.
[47] J. Maziero, L. Céleri, R. Serra, and V. Vedral, e-print arXiv:0905.3396.